

# SCIENTIFIC REPORTS



OPEN

## Limits of aerobic metabolism in cancer cells

Jorge Fernandez-de-Cossio-Diaz<sup>1</sup> & Alexei Vazquez<sup>2,3</sup> 

Cancer cells exhibit high rates of glycolysis and glutaminolysis. Glycolysis can provide energy and glutaminolysis can provide carbon for anaplerosis and reductive carboxylation to citrate. However, all these metabolic requirements could be in principle satisfied from glucose. Here we investigate why cancer cells do not satisfy their metabolic demands using aerobic biosynthesis from glucose. Based on the typical composition of a mammalian cell we quantify the energy demand and the OxPhos burden of cell biosynthesis from glucose. Our calculation demonstrates that aerobic growth from glucose is feasible up to a minimum doubling time that is proportional to the OxPhos burden and inversely proportional to the mitochondria OxPhos capacity. To grow faster cancer cells must activate aerobic glycolysis for energy generation and uncouple NADH generation from biosynthesis. To uncouple biosynthesis from NADH generation cancer cells can synthesize lipids from carbon sources that do not produce NADH in their catabolism, including acetate and the amino acids glutamate, glutamine, phenylalanine and tyrosine. Finally, we show that cancer cell lines have an OxPhos capacity that is insufficient to support aerobic biosynthesis from glucose. We conclude that selection for high rate of biosynthesis implies a selection for aerobic glycolysis and uncoupling biosynthesis from NADH generation.

Cancer cells exhibit high rates of glucose fermentation to lactate even when growing in aerobic conditions, a phenotype known as aerobic glycolysis or the Warburg effect. The Warburg effect is accompanied by other metabolic alterations, particularly increased glutamine utilization<sup>1–4</sup> and reductive carboxylation of glutamine to the lipid precursor AcCoA<sup>5</sup>. More recently, acetate has been shown to be another important source of AcCoA in cancer cells<sup>6–9</sup> and its contribution increases under oxygen limitation<sup>6</sup>.

Given that fermentation of glucose is the default pathway under anaerobic growth, Warburg originally thought that aerobic glycolysis should be rooted on mitochondrial defects<sup>10,11</sup>. However, cells from healthy mammalian tissues also manifest aerobic glycolysis and glutaminolysis during fast growth<sup>12–15</sup>. Furthermore, aerobic glycolysis is observed with concomitant high rates of respiratory metabolism in cancer<sup>15</sup> and muscle<sup>16</sup> cells.

Quantitative models of cell metabolism have been used to investigate the cause of aerobic glycolysis and related metabolic phenotypes. The postulation of a maximum oxygen consumption rate results in model predictions mimicking aerobic glycolysis in yeast<sup>17</sup> and the Warburg effect (unpublished data). However, under aerobic conditions, further increase of the oxygenation level does not abrogate aerobic glycolysis<sup>16,18</sup>. Simulations of genome scale models of mammalian cell metabolism also predict the utilization of glutamine at high proliferation rates<sup>19,20</sup>. However, we do not understand what aspects of the model are responsible for that prediction.

### Results

**OxPhos burden of aerobic growth from glucose.** To gain a better understanding of cell metabolism as a function of the growth metabolic demand we performed a back-of-the-envelope calculation focusing on the major biomass components of mammalian cells. The dry weight of mammalian cells is mostly composed of protein, lipids and polysaccharides (Table 1). Based on this composition we can estimate the biosynthetic demand for precursor metabolites and the energy that is necessary to duplicate the cell content. The duplication of a typical mammalian cell requires about 1.1 mol/L of amino acids for protein synthesis, 1.2 mol/L of AcCoA for lipid synthesis and an energy demand of  $b_{\text{demand}} = 6.0$  mol/L of ATP (Table 1).

The synthesis of biomass precursors from glucose makes use of different dehydrogenases producing/consuming NADH (Fig. 1). The synthesis of some amino acids involves transamination coupled with glutamate to  $\alpha$ -ketoglutarate conversion.  $\alpha$ -ketoglutarate can be converted back to glutamate via reverse glutamate

<sup>1</sup>Center of Molecular Immunology, Havana, Cuba. <sup>2</sup>Cancer Research UK Beatson Institute, Glasgow, UK. <sup>3</sup>Institute for Cancer Sciences, University of Glasgow, Glasgow, UK. Correspondence and requests for materials should be addressed to A.V. (email: [a.vazquez@beatson.gla.ac.uk](mailto:a.vazquez@beatson.gla.ac.uk))

Biomass component (% of dry weight)		Precursor demand (mol/L cell)		Energy demand $b_{demand}$ (mol ATP/L cell)	NADH OxPhos $b_{coupled}$ (mol ATP/L cell)
Protein	60	Amino acids	1.10	4.62	1.57
Lipids	16.7	AcCoA	1.19	1.04	5.95
Polysaccharides	6.7	Glucose	0.07	0.15	0
RNA	3.7	Ribonucl.	0.02	0.11	0.06
DNA	0.8	Deoxyribonucl.	0.01	0.03	0.01
Total				6.0	7.6

**Table 1.** Growth requirements. Composition and growth requirements of a typical mammalian cell. The NADH OxPhos column reports the energy that can be generated coupled to OxPhos of the NADH produced by biosynthetic pathways from glucose.

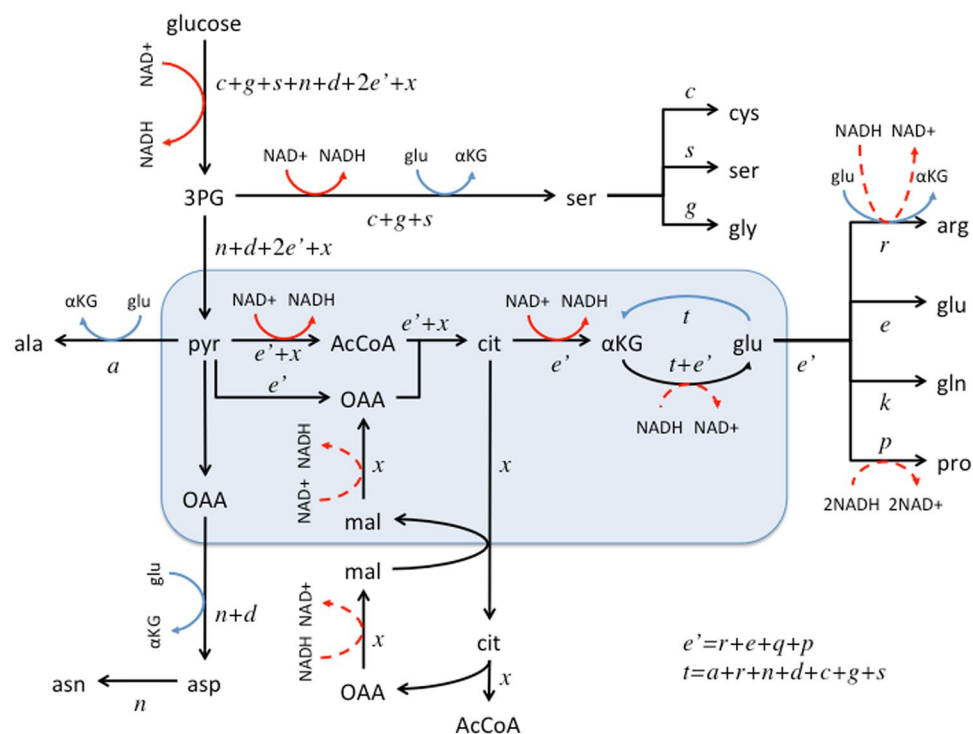


**Figure 1.** Biosynthesis from glucose. Synthesis of precursor metabolites from glucose. The text in italics represents the precursor requirements to duplicate a cell, using the one letter nomenclature for amino acids and  $x$  for AcCoA. Dehydrogenase steps are highlighted with red arrows (solid forward and dashed reverse) and transaminase steps with blue arrows. ATP and other cofactors have been omitted for simplicity.

dehydrogenase consuming NADH. When all these contributions are taken into account we obtain a net production of NADH coupled to the biosynthesis of precursor metabolites from glucose. The NADH produced can be oxidized in the mitochondria coupled to ATP generation. Assuming a 2.5 ATP/NADH yield we obtain that mammalian cells can produce  $b_{coupled} = 7.6$  mol ATP/L coupled to NADH production by biosynthetic pathways (NADH OxPhos, Table 1).

The aerobic biosynthesis of a cell from glucose relies on the capacity of mitochondria to generate the energy required for biosynthesis and to oxidize the NADH generated through biosynthesis. In the following we calculate how fast a cell can proliferate given a specified mitochondrial content. If  $a$  is the growth-independent energy demand for cell maintenance,  $b$  is the OxPhos demand to duplicate the cell content,  $T$  is the cell doubling time,  $r_M$  is the OxPhos capacity of mitochondria (mol ATP/L of mitochondria) and  $\phi_M$  is the mitochondria volume fraction (L mitochondria/L cell) then the following constraint must be satisfied

$$a + b \frac{\ln 2}{T} \leq r_M \phi_M \quad (1)$$

If cells proliferate too fast, shortening the doubling time (left hand side of equation 1), they will overcome the maximum OxPhos capacity (right hand side of equation 1). From equation 1 we can determine the minimum doubling time that is supported by aerobic biosynthesis from glucose

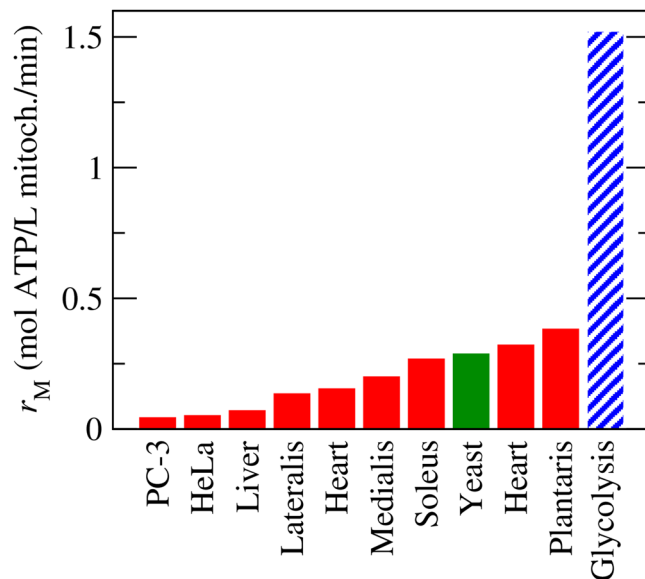


**Figure 2.** Mitochondria capacity. Mitochondria intrinsic capacity (per volume of mitochondria) for ATP generation, based on data reported in the literature (Supplementary Table S2). Red represents data for different mammalian tissues and cell lines. Green represents data for yeast. As a reference, in dashed-blue we highlight the intrinsic capacity of glycolysis.

$$T_{\min} = \frac{b \ln 2}{r_M \phi_M - a} \quad (2)$$

The mitochondria OxPhos capacity ( $r_M$ ) has been measured for isolated mitochondria (Fig. 2 and Supplementary Table S2). It can be as high as 0.38 mol ATP/L mitochondria/min in muscle cells. The mitochondria of yeast cells is as efficient, with  $r_M = 0.29$  mol ATP/L mitochondria/min. However, the mitochondria of cancer cells is 10 fold less efficient, with  $r_M = 0.042$ – $0.068$  mol ATP/L mitochondria/min.

**Growth phases.** As discussed above, even with mitochondria working at maximum capacity, a limited mitochondria content results in a limited oxidative phosphorylation capacity for both energy generation and NADH oxidation. What remains to be determined is whether such limitation is relevant when the actual mitochondria content and energy demand of cells are taken into consideration. To this end in Fig. 3 we depict the different scenarios that can occur depending on mitochondria content, maintenance energy and doubling time, as implied by equation (2). The top right corner corresponds with a growth phase where cells can proliferate producing all the energy from OxPhos and can synthesize precursor metabolites from glucose (facultative OxPhos and facultative coupling of biosynthesis to NADH production, FF phase). We notice that “they can” does not imply “they must”. A cell line may have a doubling time and mitochondria content in that region, but it may have up-regulated aerobic glycolysis due to genetic alterations. Cells may also utilize alternative carbon sources due to overexpression of transport systems, reducing the NADH production coupled to biosynthesis. In such cases we can truly speak of an inefficient/wasteful/accidental phenotype. The other extreme is the grey zone highlighted in Fig. 3, where the energy demand associated with cell maintenance exceeds the OxPhos capacity ( $a > r_M \phi_M$  in equation 2). In this region cells cannot survive without activating aerobic glycolysis.

In mammalian cells the energy that can be generated from OxPhos of the NADH produced in biosynthetic pathways exceeds the energy demand of biosynthesis ( $b_{\text{demand}} < b_{\text{coupled}}$ , Table 1). As cells decrease their doubling time and/or decrease their mitochondrial content, they will first be limited by the inability of mitochondria to turnover the NADH produced coupled to the biosynthesis of precursor metabolites (Fig. 3, red-dashed line). To proliferate faster, shortening the doubling time, mammalian cells need to uncouple NADH production from the synthesis of precursor metabolites (facultative OxPhos and obligatory uncoupling of biosynthesis from NADH production, FO phase). In the FO phase mammalian cells can satisfy their energy demand from OxPhos, until the energy demand of biosynthesis reaches the OxPhos capacity (Fig. 3, black-solid line). Below the black-solid line mammalian cells cannot satisfy their energy demand using OxPhos and they must switch on aerobic glycolysis (obligatory aerobic glycolysis and obligatory uncoupling of biosynthesis from NADH production, OO phase). In this case aerobic glycolysis is not an inefficient/wasteful/accidental phenotype, it is the only choice left to proliferate faster.

To determine the location of cancer cells in the growth phase diagram of Fig. 3, we focus on the NCI60 panel of tumour derived cell lines. The doubling times for these cell lines has been reported by the NCI Developmental Therapeutics Program and we have estimated their mitochondrial content. Each cross in Fig. 3 represents a cell line in the NCI60 panel. Most cell lines fall in the grey area, where OxPhos cannot supply the energy requirements of cell maintenance and aerobic glycolysis must be activated. Indeed, these cell lines convert approximately 70% of

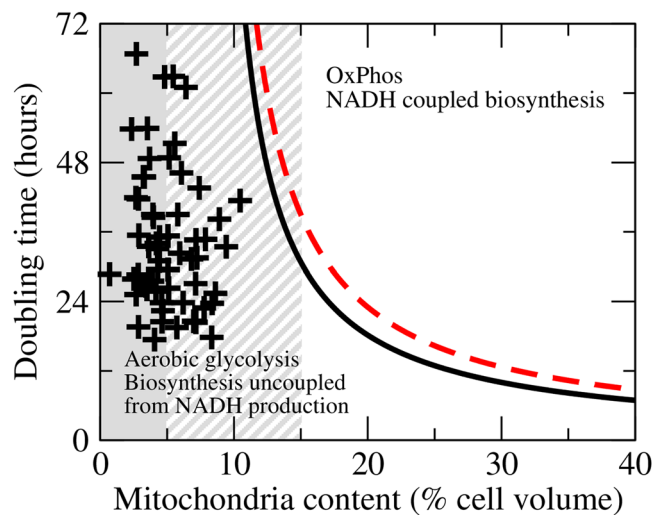


**Figure 3.** Growth phase diagram. Different growth phases as a function of the cell doubling time and mitochondrial content. The black-solid line is obtained using equation 2, setting the OxPhos demand equal to the energy demand of cell duplication ( $b = b_{\text{demand}}$ ). The red dashed line is obtained using equation 2, setting the OxPhos demand equal to the NADH OxPhos of cell duplication ( $b = b_{\text{coupled}}$ ). The grey area demarks the region where the OxPhos capacity is insufficient to satisfy the energy demand for cell maintenance, with solid and dashed patterns indicating the certain area average minus one standard deviation and uncertain area (average plus minus two standard deviations) given our current estimates of the cell maintenance. The pluses represent 60 cancer cell lines from the NCI60 panel.

the imported glucose to lactate<sup>21,22</sup>. For these cancer cells we can conclude that aerobic glycolysis is a consequence of a limited OxPhos capacity. Metabolic flux estimations indicate that these cells generate ATP from OxPhos in amounts comparable to aerobic glycolysis<sup>22</sup>. The observation of this mixed aerobic-glycolysis/OxPhos phenotype does not contradict our conclusion that aerobic glycolysis is obligatory for these cells. Simply the energy generated from OxPhos falls short of the energy demand.

**Uncoupling NADH production from biosynthesis.** Biosynthesis can be uncoupled from NADH generation in different ways. NADH can be turnover ( $\text{NADH} \rightarrow \text{NAD}^+$ ) coupled to NADPH production ( $\text{NADP}^+ \rightarrow \text{NADPH}$ ), using combinations of cytosolic/mitochondrial  $\text{NAD}^+$  and  $\text{NADP}^+$  dehydrogenases and the mitochondria transhydrogenase. We notice that the conversion of NADH to NADPH by the transhydrogenase transports protons from the mitochondria matrix to the cytosol, uncoupling OxPhos from ATP generation. Therefore, the NADH turnover by the transhydrogenase comes at expenses of exacerbating the limited OxPhos for energy production.

As an alternative, cells can switch to other carbon sources to reduce NADH production. The limited OxPhos capacity dictates which carbon sources are more suitable to uncouple NADH production from biosynthesis. Certainly for each amino acid the amino acid itself is a suitable alternative carbon source. The choice is in principle more redundant for AcCoA (Fig. 4a). Acetate can be used with the extra cost of 1 ATP for the acetyl CoA ligase step. On the other hand, the  $\beta$ -oxidation of fatty acids generates NADH and FADH<sub>2</sub> and therefore it does not reduce the NADH generation burden. AcCoA could also be produced from amino acids. However, in most cases NADH is generated (Fig. 4a, grey lines). The catabolism of isoleucine, leucine, lysine, methionine, tryptophan, and valine requires one or more dehydrogenase steps generating NADH. Alanine, cysteine, glycine, threonine and serine can be converted to pyruvate, which still requires pyruvate dehydrogenase to produce AcCoA (Fig. 1). Aspartate and asparagine can be converted to oxaloacetate, which still requires a source of AcCoA for citrate synthesis or conversion to pyruvate, again requiring pyruvate dehydrogenase to produce AcCoA. Finally, arginine and proline can be converted to glutamate but NADH is generated in the process.

There are only two groups of amino acids that can be converted to citrate without NADH production. The first group includes glutamate and glutamine. Glutamate can be converted to citrate via reductive carboxylation. In this pathway the NAD(P)H production by glutamate dehydrogenase is compensated by the reverse activity of the NAD(P) isocitrate dehydrogenase (Fig. 1). Glutamate can be taken from the medium or generated from glutamine by glutaminase. Interestingly, arginine and proline can be produced from glutamate with concomitant consumption of NADH (Fig. 4a). This could provide an additional mechanism for NADH turnover. The second group is composed of the amino acids phenylalanine and tyrosine, which are converted to acetoacetate and fumarate (Fig. 4a). Acetoacetate yields 2 AcCoA *via* the combined activity of acetoacetate CoA ligase (consuming one ATP) and acetyl-CoA transferase. Fumarate on the other hand is better excreted to avoid additional OxPhos burden. We notice that the catabolism of phenylalanine and tyrosine to acetoacetate consumes 3 and 2 oxygen molecules respectively. Therefore, these amino acids are not suitable to uncouple NADH production from biosynthesis under hypoxia.

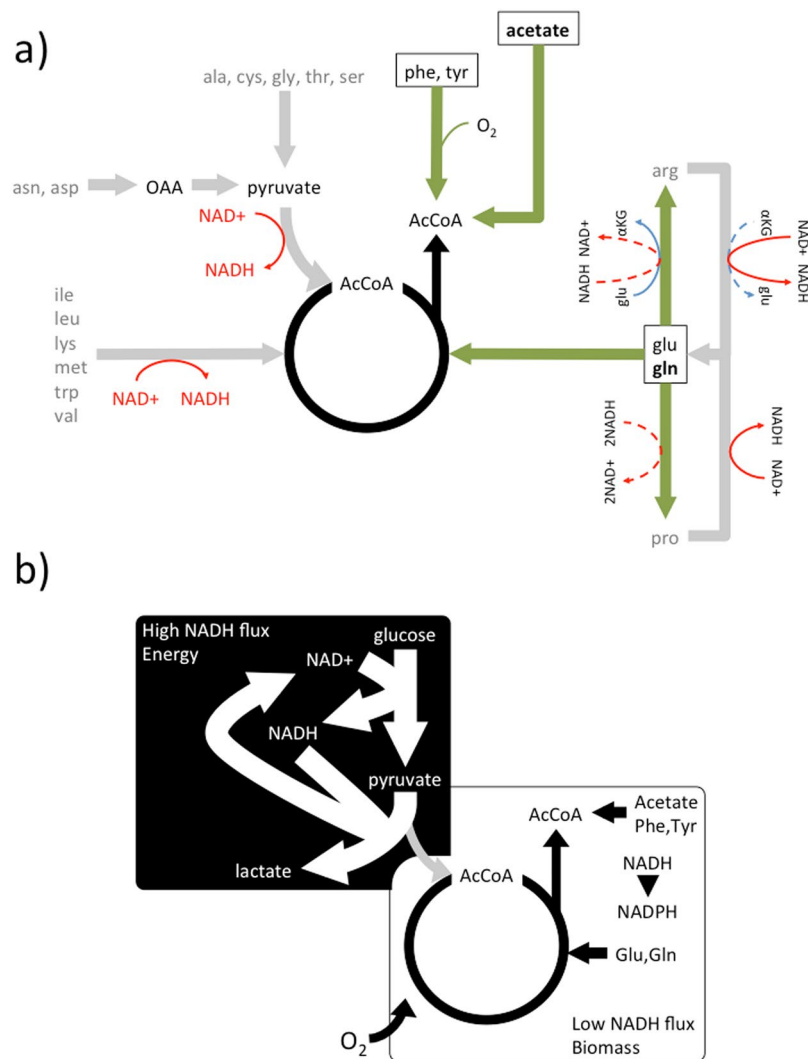


**Figure 4.** Metabolism under a limited OxPhos capacity. (a) Synthesis of AcCoA from alternative carbon sources. In grey we highlight carbon sources that result in NADH production. The boxes highlight the carbon sources that uncouple AcCoA synthesis from NADH production. (b) Compartmentalization of eukaryote aerobic cell metabolism in the context of a limited OxPhos capacity.

**NADPH production.** For the sake of simplicity we have omitted the balance of some key co-factors that are also required for cell proliferation. NADPH is a free energy source required in the biosynthesis of some amino acids and of lipids. The pentose phosphate pathway (PPP) is a major source of NADPH production. The PPP is interconnected with the upper part of glycolysis, above the glyceraldehyde 3-phosphate dehydrogenase step. Therefore, the PPP does not change the pyruvate/NADH yield ratio of glycolysis, which is the only feature of glycolysis used to calculate the biosynthetic requirements reported in Table 1. The increase in the NADPH yield just reduces the percentage of glucose carbons incorporated into biomass (1 CO<sub>2</sub> molecule is released per every 2 NADPH).

NADPH can also be produced *via* one-carbon metabolism using serine as the one-carbon source<sup>23,24</sup>. The synthesis of serine from glucose generates NADH (Fig. 1). Therefore the glucose → serine → one-carbon pathway of NADPH generation is only suitable when cells have not reached their maximum OxPhos capacity. When cells have overcome their OxPhos capacity they could import serine from the media to uncouple NADH production from NADPH production via one-carbon metabolism. To donate the one-carbon unit serine is converted to glycine and glycine could also donate a one-carbon unit *via* the glycine cleavage system. The glycine cleavage system generates NADH and therefore this pathway is only suitable when cells have not reached their maximum OxPhos capacity. Otherwise, glycine is better excreted to avoid additional NADH production.

## Discussion

When the metabolic demand exceeds the limited OxPhos capacity mammalian cells split their metabolism into two major components (Fig. 4b). There is a component of high NADH flux from aerobic glycolysis (Fig. 4b, black background box). The function of this component is to satisfy the energy demand beyond the OxPhos capacity.



There is another component of low NADH flux where precursor metabolites are produced from glucose and other carbon sources (Fig. 4b, white background box). The function of this component is to generate precursor metabolites with the minimal NADH generation that can be absorbed by the limited OxpHos capacity. The choice of alternative carbon sources is restricted to those that do not generate NADH in their conversion to precursor metabolites. For generation of AcCoA, this constraint leave cells with the choice of acetate and the amino acids glutamate, glutamine, phenylalanine and tyrosine.

In the context of cancer metabolism it has been often claimed that aerobic glycolysis is a consequence of an increased demand of carbon atoms for biosynthesis of precursor metabolites<sup>25,26</sup>. A more precise statement is that the increased demand for carbon atoms results in an increased demand for NADH turnover when glucose is the carbon source. However, the excretion of lactate does not solve the problem of NADH production coupled to biosynthesis. While it is true that lactate dehydrogenase converts NADH back to NAD<sup>+</sup>, the carbon atoms associated with this conversion are excreted as lactate and they do not contribute to the formation of biomass precursors. We conclude, as originally postulated by Warburg and supported by previous calculations<sup>27</sup>, that the role of aerobic glycolysis is to satisfy the energy demand in the context of limited mitochondria OxPhos capacity.

These conclusions will hold up to small variations in the parameter values required for the analysis. Imprecisions in the demand of energy and NADH turnover may cause a change in the order of the continuous and dashed lines in Fig. 3, but the two phases at the top-right and bottom-left corners will remain. The intrinsic mitochondria efficiency of cancer cells may be larger than the values obtained for PC-3 and HeLa cells, causing some cell lines to fall in the growth phase where aerobic glycolysis is not obligatory. Therefore, our conclusion of aerobic glycolysis being obligatory may not necessarily hold for all cancer cells. In spite of these potential issues, this analysis provides a conceptual framework that brings together apparently disconnected metabolic phenotypes of cancer cells.

## Methods

**Cell composition.** The typical biomass composition of mammalian cells was obtained from ref.<sup>28</sup>. The typical composition in terms of precursor metabolites (mol of precursor/L cell) was calculated using the equation

$$c = \frac{\pi}{\mu v_{s,cell}} \quad (3)$$

where  $\pi$  is the dry weight fraction of the biomass component,  $\mu$  is the molecular weight of the precursor metabolite and  $v_{s,cell}$  is the cell specific volume (L cell/g dry weight). Amino acids are the precursor metabolites of proteins. The average molecular weight of an amino acid in expressed proteins is  $\mu_{aa} = 109$  g/mol in mammalian cells<sup>29</sup>. The acetyl group of AcCoA is the precursor of lipids. Its average molecular weight in lipids was estimated as two times the molecular weight of CH<sub>2</sub> ( $\mu_{ac} = 28$  g/mol). Ribonucleotides are the precursor metabolites of RNA. The average molecular weight of a ribonucleotide in expressed RNAs is  $\mu_{rn} = 331$  g/mol in mammalian cells<sup>29</sup>. Deoxyribonucleotides are the precursor metabolites of DNA. The average molecular weight of a deoxyribonucleotide in expressed DNA is  $\mu_{dn} = 332$  g/mol in mammalian cells<sup>29</sup>. Finally, the cell specific volume is 5 mL/gDW for mammalian cells<sup>30</sup>.

**Energy requirements of biosynthesis.** The mammalian cell energy requirement for synthesis of each biomass component from glucose was estimated as the number of ATP molecules required to synthesize the precursor from glucose, based on reported biosynthesis pathways<sup>31</sup>, plus the energy required for polymerization<sup>29</sup>, times the precursor concentration (Supplementary Table S1).

**NADH OxPhos.** The number of NADH molecules produced coupled to the synthesis of each precursor metabolite from glucose was calculated from reported biosynthesis pathways<sup>31</sup>. This value was multiplied by a yield of 2.5 ATP/NADH times the precursor concentration reported in Table 1 (see also Supplementary Table S1).

**Mitochondria OxPhos capacity.** The mitochondria OxPhos capacity  $r_M$  was obtained from literature reports (Supplementary Table S2).

**Maintenance energy.** We have estimated the cell maintenance energy of cancer cells using literature reports of extracellular acidification rates (ECAR) and oxygen consumption rates (OCR) quantified using the Seahorse instrument (Table S3). The ECAR and OCR measurements were then converted to energy production from glycolysis and OxPhos using the protocol reported in reference {Mookerjee, 2017 #7479}. The energy maintenance was estimated as the total energy production (glycolysis + OxPhos) minus the energy requirements of growth ( $6 \text{ mol ATP/L cell} \times \ln 2/T_d$ ). The average and standard deviation across cell lines was used to calculate the shadow areas in Fig. 3. The average value across cell lines was 5 mmol ATP/L cell/min, no far from an estimated based on data reported for the LS mouse cell line<sup>32</sup>. LS mouse cells require 17 pmol ATP/cell/day for cell maintenance. Dividing by the LS cell volume (3.4 pL/cell) we obtain the cell maintenance energy demand per cell volume  $a_{mammalian} = 3.5 \text{ mmol ATP/L cell/min}$ .

**NCI60.** The doubling times for each cell line are reported by the NCI Developmental Therapeutics Program [https://dtp.cancer.gov/discovery\\_development/nci-60/cell\\_list.htm](https://dtp.cancer.gov/discovery_development/nci-60/cell_list.htm). Their mitochondrial content was estimated as

$$\phi_M = \frac{P_{cell} v_{s,mitochondria}}{V_{cell}} \frac{\sum_i p_i l_i}{\sum_i p_i} \quad (4)$$

where  $P_{cell}$  is the protein content (g/cell),  $V_{cell}$  is the cell volume (L/cell),  $v_{s,mitochondria}$  is the mitochondrial specific volume (L/g mitochondrial protein), the sums run over all expressed proteins,  $p_i$  is the abundance of each protein and  $l_i = 1$  if the protein localizes to the mitochondria and 0 otherwise.  $P_{cell}$  and  $V_{cell}$  are reported in ref.<sup>22</sup>. The mitochondria specific volume is  $v_{s,mitochondria} = 2.6$  mL/g mitochondrial protein<sup>33</sup>. The relative protein abundances were obtained from reported proteomic data<sup>34</sup>. The protein localization we obtained from the NCBI annotations.  $l_i$  was set to 1 for every protein that is annotated to localize to the mitochondria. The estimated mitochondria content is reported in the Supplementary Table S4.

## References

- Eagle, H. Nutrition Needs of Mammalian Cells in Tissue Culture. *Science* **122**, 501–504 (1955).
- Sauer, L. A. & Dauchy, R. T. Ketone body, glucose, lactic acid, and amino acid utilization by tumors *in vivo* in fasted rats. *Cancer Res* **43**, 3497–3503 (1983).
- Sauer, L. A., Stayman, J. W. 3rd & Dauchy, R. T. Amino acid, glucose, and lactic acid utilization *in vivo* by rat tumors. *Cancer Res* **42**, 4090–4097 (1982).
- DeBerardinis, R. J. *et al.* Beyond aerobic glycolysis: transformed cells can engage in glutamine metabolism that exceeds the requirement for protein and nucleotide synthesis. *Proc Natl Acad Sci USA* **104**, 19345–19350 (2007).
- Mullen, A. R. *et al.* Reductive carboxylation supports growth in tumour cells with defective mitochondria. *Nature* **481**, 385–388 (2012).
- Kamphorst, J. J., Chung, M. K., Fan, J. & Rabinowitz, J. D. Quantitative analysis of acetyl-CoA production in hypoxic cancer cells reveals substantial contribution from acetate. *Cancer & metabolism* **2**, 23 (2014).
- Comerford, S. A. *et al.* Acetate Dependence of Tumors. *Cell* **159**, 1591–1602 (2014).
- Mashimo, T. *et al.* Acetate Is a Bioenergetic Substrate for Human Glioblastoma and Brain Metastases. *Cell* **159**, 1603–1614 (2014).
- Schug, Z. T. *et al.* Acetyl-CoA Synthetase 2 Promotes Acetate Utilization and Maintains Cancer Cell Growth under Metabolic Stress. *Cancer cell* **27**, 57–71 (2015).
- Warburg, O. On respiratory impairment in cancer cells. *Science* **124**, 269–270 (1956).
- Warburg, O. On the origin of cancer cells. *Science* **123**, 309–314 (1956).
- Wang, T., Marquardt, C. & Foker, J. Aerobic glycolysis during lymphocyte proliferation. *Nature* **261**, 702–705 (1976).
- Brand, K. Glutamine and glucose metabolism during thymocyte proliferation. *Pathways of glutamine and glutamate metabolism. Biochem J* **228**, 353–361 (1985).
- Newsholme, E. A., Crabtree, B. & Ardawi, M. S. Glutamine metabolism in lymphocytes: its biochemical, physiological and clinical importance. *Q J Exp Physiol* **70**, 473–489 (1985).
- Zu, X. L. & Guppy, M. Cancer metabolism: facts, fantasy, and fiction. *Biochemical and biophysical research communications* **313**, 459–465 (2004).
- Kemper, W. F., Lindstedt, S. L., Hartzler, L. K., Hicks, J. W. & Conley, K. E. Shaking up glycolysis: Sustained, high lactate flux during aerobic rattling. *Proc Natl Acad Sci USA* **98**, 723–728 (2001).
- Famili, I., Forster, J., Nielsen, J. & Palsson, B. O. *Saccharomyces cerevisiae* phenotypes can be predicted by using constraint-based analysis of a genome-scale reconstructed metabolic network. *Proc Natl Acad Sci USA* **100**, 13134–13139 (2003).
- Conley, K. E., Kushmerick, M. J. & Jubrias, S. A. Glycolysis is independent of oxygenation state in stimulated human skeletal muscle *in vivo*. *The Journal of physiology* **511**(Pt 3), 935–945 (1998).
- Shlomi, T., Benyamini, T., Gottlieb, E., Sharan, R. & Ruppin, E. Genome-scale metabolic modeling elucidates the role of proliferative adaptation in causing the warburg effect. *Plos Comput Biol* **7**, e1002018 (2011).
- Vazquez, A. & Oltvai, Z. N. Molecular crowding defines a common origin for the warburg effect in proliferating cells and the lactate threshold in muscle physiology. *Plos One* **6**, e1953 (2011).
- Jain, M. *et al.* Metabolite profiling identifies a key role for glycine in rapid cancer cell proliferation. *Science* **336**, 1040–1044 (2012).
- Dolfi, S. C. *et al.* The metabolic demands of cancer cells are coupled to their size and protein synthesis rates. *Cancer & metabolism* **1**, 20 (2013).
- Tedeschi, P. M. *et al.* Contribution of serine, folate and glycine metabolism to the ATP, NADPH and purine requirements of cancer cells. *Cell Death & Disease* **4**, e877 (2013).
- Fan, J. *et al.* Quantitative flux analysis reveals folate-dependent NADPH production (vol 510, pg 298, 2014). *Nature* **513**, 574–574 (2014).
- Vander Heiden, M. G., Cantley, L. C. & Thompson, C. B. Understanding the Warburg effect: the metabolic requirements of cell proliferation. *Science* **324**, 1029–1033 (2009).
- Lunt, S. Y. & Vander Heiden, M. G. Aerobic glycolysis: meeting the metabolic requirements of cell proliferation. *Annual review of cell and developmental biology* **27**, 441–464 (2011).
- Vazquez, A., Liu, J., Zhou, Y. & Oltvai, Z. N. Catabolic efficiency of aerobic glycolysis: The Warburg effect revisited. *Bmc Syst Biol* **4**, 58 (2010).
- Alberts, B. *Molecular biology of the cell*. 5th edn, (Garland Science, 2008).
- Sheikh, K., Forster, J. & Nielsen, L. K. Modeling hybridoma cell metabolism using a generic genome-scale metabolic model of *Mus musculus*. *Biotechnol Prog* **21**, 112–121 (2005).
- Frame, K. K. & Hu, W. S. Cell volume measurement as an estimation of mammalian cell biomass. *Biotechnol Bioeng* **36**, 191–197 (1990).
- Voet, D. & Voet, J. G. *Biochemistry*. 4th edn, (John Wiley & Sons, Inc., 2011).
- Kilburn, D. G., Lilly, M. D. & Webb, F. C. The energetics of mammalian cell growth. *Journal of Cell Science* **4**, 645–654 (1969).
- Schwerzmann, K., Hoppeler, H., Kayar, S. R. & Weibel, E. R. Oxidative capacity of muscle and mitochondria: correlation of physiological, biochemical, and morphometric characteristics. *Proc Natl Acad Sci USA* **86**, 1583–1587 (1989).
- Moghaddas Gholami, A. *et al.* Global Proteome Analysis of the NCI-60 Cell Line Panel. *Cell Rep* **4**, 609–620 (2013).

## Acknowledgements

This work was supported by Cancer Research UK C596/A21140. This project has received funding from the European Union's Horizon 2020 research and innovation programme MSCA-RISE-2016 under grant agreement No. 734439 INFERNET.

## Author Contributions

J.F.C.D. and A.V. performed the calculations and wrote the manuscript.

## Additional Information

Supplementary information accompanies this paper at <https://doi.org/10.1038/s41598-017-14071-y>.

**Competing Interests:** The authors declare that they have no competing interests.

**Publisher's note:** Springer Nature remains neutral with regard to jurisdictional claims in published maps and institutional affiliations.



**Open Access** This article is licensed under a Creative Commons Attribution 4.0 International License, which permits use, sharing, adaptation, distribution and reproduction in any medium or format, as long as you give appropriate credit to the original author(s) and the source, provide a link to the Creative Commons license, and indicate if changes were made. The images or other third party material in this article are included in the article's Creative Commons license, unless indicated otherwise in a credit line to the material. If material is not included in the article's Creative Commons license and your intended use is not permitted by statutory regulation or exceeds the permitted use, you will need to obtain permission directly from the copyright holder. To view a copy of this license, visit <http://creativecommons.org/licenses/by/4.0/>.

© The Author(s) 2017